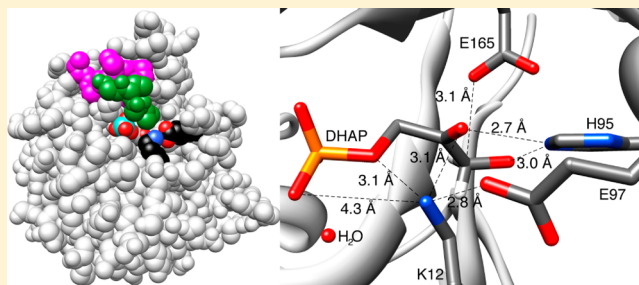


A Paradigm for Enzyme-Catalyzed Proton Transfer at Carbon: Triosephosphate Isomerase

John P. Richard*

Department of Chemistry, University at Buffalo, State University of New York, Buffalo, New York 14260-3000, United States

ABSTRACT: Triosephosphate isomerase (TIM) catalyzes the stereospecific 1,2-proton shift at dihydroxyacetone phosphate (DHAP) to give (*R*)-glyceraldehyde 3-phosphate through a pair of isomeric enzyme-bound *cis*-enediolate phosphate intermediates. The chemical transformations that occur at the active site of TIM were well understood by the early 1990s. The mechanism for enzyme-catalyzed isomerization is similar to that for the nonenzymatic reaction in water, but the origin of the catalytic rate acceleration is not understood. We review the results of experimental work that show that a substantial fraction of the large 12 kcal/mol intrinsic binding energy of the nonreacting phosphodianion fragment of TIM is utilized to activate the active site side chains for catalysis of proton transfer. Evidence is presented that this activation is due to a phosphodianion-driven conformational change, the most dramatic feature of which is closure of loop 6 over the dianion. The kinetic data are interpreted within the framework of a model in which activation is due to the stabilization by the phosphodianion of a rare, desolvated, loop-closed form of TIM. The dianion binding energy is proposed to drive the otherwise thermodynamically unfavorable desolvation of the solvent-exposed active site. This reduces the effective local dielectric constant of the active site, to enhance stabilizing electrostatic interactions between polar groups and the anionic transition state, and increases the basicity of the carboxylate side chain of Glu-165 that functions to deprotonate the bound carbon acid substrate. A rebuttal is presented to the recent proposal [Samanta, M., Murthy, M. R. N., Balam, H., and Balam, P. (2011) *ChemBioChem* 12, 1886–1895] that the cationic side chain of K12 functions as an active site electrophile to protonate the carbonyl oxygen of DHAP.



The contradiction between the perception that X-ray crystal structures of enzymes place in plain view everything needed to explain their catalytic rate acceleration and the reality that there are substantial gaps in our understanding of enzyme catalysis is apparent when considering the complex problem of designing proteins with enzymatic activity.¹ We need to improve our understanding of the explanation for enzymatic rate accelerations, and the best way to move forward is to focus on enzymes with well-understood mechanisms.

Triosephosphate isomerase (TIM) catalyzes the stereospecific 1,2-proton shift at dihydroxyacetone phosphate (DHAP) to give (*R*)-glyceraldehyde 3-phosphate through a pair of isomeric enzyme-bound *cis*-enediolate phosphate reaction intermediates (Scheme 1).² The enzyme's high cellular abundance,³ low molecular mass (dimer of 26 kDa/subunit), prominent role in the 4 billion year old glycolytic pathway,⁴ and the centrality of proton transfer reactions at carbon⁵ in metabolism⁶ have made TIM a prominent target for mechanistic studies.^{2,7,8} Jeremy Knowles and Greg Petsko established a fruitful collaboration through the 1980s and into the 1990s that combined X-ray crystallography with emerging technology for the preparation of site-directed mutant enzymes. An important result of this work was to establish the chemical mechanism for isomerization at the enzyme active site (Figure 1). Catalysis proceeds by deprotonation of the enzyme-bound substrate using the carboxylate side chain of Glu-165 (the

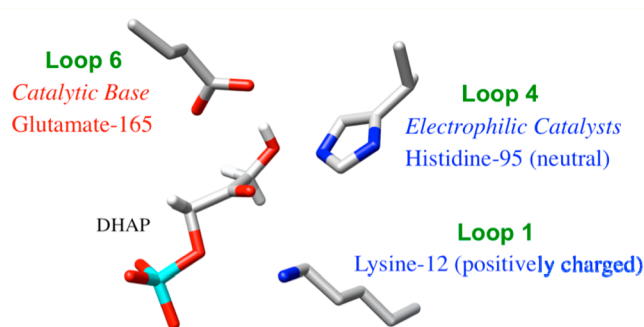


Figure 1. Orientation of the catalytic side chains at the active site of TIM (PDB entry 1NEY).⁵⁴ The carboxylate side chain of E165 found at the front of flexible loop 6 is positioned to deprotonate the carbon acid substrate of DHAP. The neutral imidazole side chain of H95, which is part of loop 4, is positioned to form hydrogen bonds to O-1 or O-2 of isomeric enediolate phosphate reaction intermediates. The cationic side chain of K12, which is part of loop 1, forms an ion pair to the phosphodianion of the substrate.

numbering is for the sequence of TIM from chicken muscle, unless indicated otherwise)^{9,10} in a reaction assisted by the

Received: February 13, 2012

Revised: March 7, 2012

Published: March 12, 2012

Scheme 1

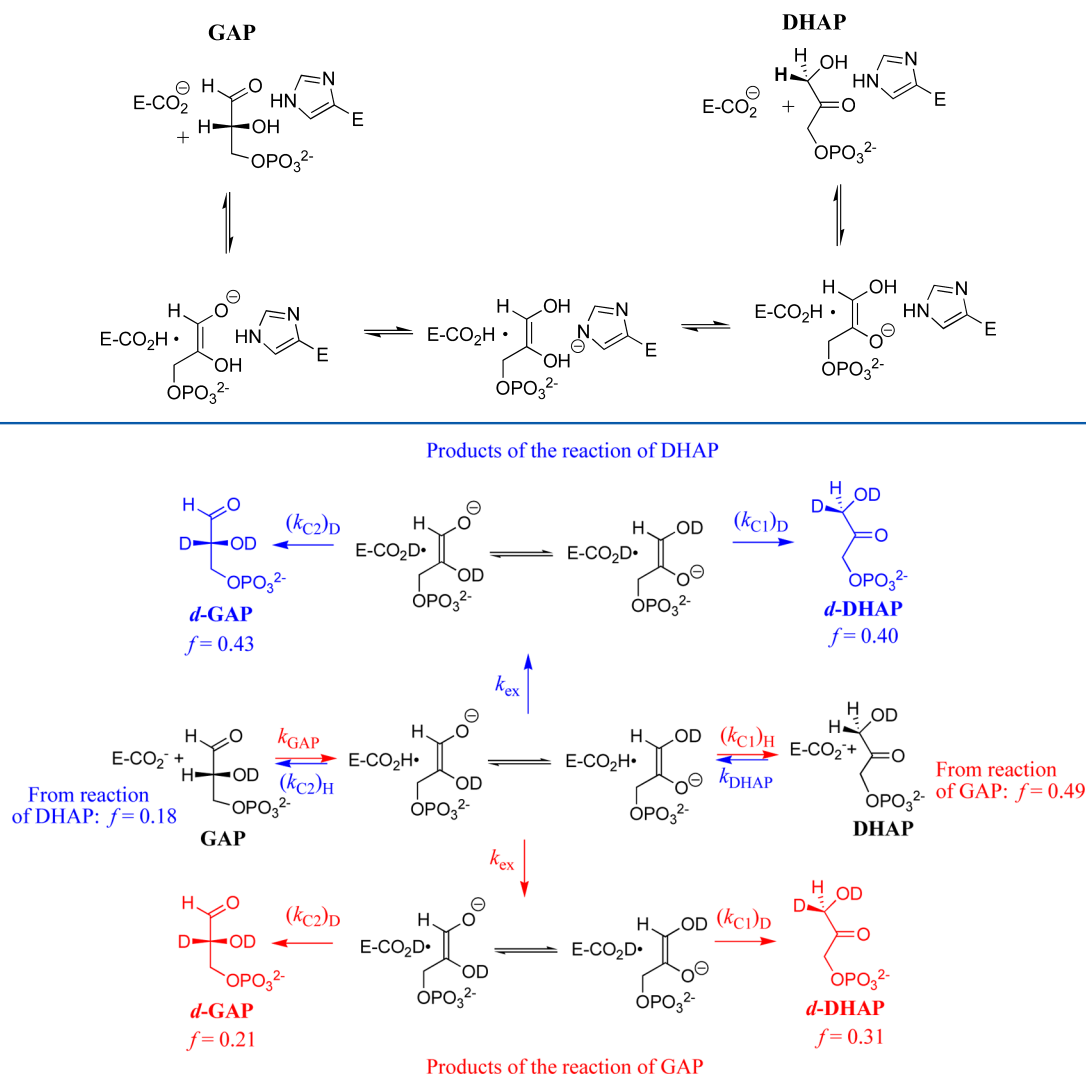


Figure 2. Pathways for formation of the products of the TIM-catalyzed reactions of GAP and DHAP in D₂O. The yields of the products of the reaction of GAP are colored red, and the yields of the products of the reaction of DHAP are colored blue.

neutral imidazole side chain of His-95.¹¹ The alkylammonium side chain of Lys-12 was shown to play an important but poorly defined role in providing electrostatic stabilization of the bound substrate dianion.^{12,13} A pair of elegant and optimistic reviews^{14,15} from 1991 summarized the many aspects of the reaction mechanism that were well understood, while explaining problems that required additional study.

Only 40 years ago there was a sense of mystery attached to the mechanism of enzyme catalysis and excitement as X-ray crystal structures exposed the interiors of these catalytic black boxes. The collaborative studies of Knowles and Petsko on TIM had an uplifting influence on me and other mechanistic enzymologists. However, the chemical reaction mechanism for TIM (Figure 1) is not significantly different from that for nonenzymatic isomerization in water.¹⁶ The detailed active site structures provide limited guidance for catalyst design, beyond proposals that catalytic side chains should be tethered at a binding pocket, which is complementary to the substrate. However, these side chains must in some sense be activated for catalysis at the enzyme active site compared to water, and there is no general agreement about the mechanisms for this

activation. We summarize here our mechanistic studies of this problem of enzyme activation.

TIM-Catalyzed Hydron Transfer. The partitioning of tracer levels of tritium in the solvent water and at the substrate [1(R)-³H]DHAP was monitored in transformative studies to define the relative barriers to the microscopic steps for TIM-catalyzed isomerization.⁷ We showed many years later that high-resolution ¹H NMR spectroscopy is a powerful analytical method for monitoring nonenzymatic proton transfer reactions at carbon in D₂O.^{17–22} This technique is well suited for studies on the mechanism of action of TIM. It has the advantage over studies with tritium of providing directly the yields of the products of hydron transfer, without the requirement for separation of the labeled hydron in products from that in the unreacted substrate.

We have examined TIM-catalyzed deprotonation of GAP²³ or DHAP²⁴ in D₂O. These reactions proceed through isomeric enediolate intermediates that partition between intramolecular transfer of ¹H to product and irreversible exchange of the ¹H-labeled enzyme with deuterium from solvent to give ²H-labeled enzyme which, in turn, partitions to form *d*-GAP and *d*-DHAP

(Figure 2). The product yields summarized in Figure 2 provided support for several important conclusions from earlier work with tritium at tracer levels in solvent or $[1(R)\text{-}^3\text{H}]\text{DHAP}$ but raised questions about the following simplifying assumptions made in interpreting these earlier results.^{23,24}

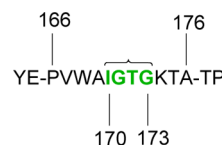
(1) The transfer of hydron between bulk solvent and TIM was assumed to be fast relative to turnover, so that the ^1H - and ^3H -labeled carboxylic acid side chains of Glu-165 “are essentially at equilibrium”.⁷ Exchange of ^3H is fast relative to turnover, as shown by the nearly complete ($\approx 95\%$) wash out of tritium during the irreversible conversion of $[1(R)\text{-}^3\text{H}]\text{-DHAP}$ to GAP in H_2O . TIM-catalyzed isomerization of $[2(R)\text{-}^3\text{H}]\text{GAP}$ was not examined in these earlier studies. Our observation that the TIM-catalyzed reaction of GAP in D_2O gives a 49% yield of DHAP from a reaction with intramolecular transfer of hydrogen²³ shows that $k_{\text{ex}} \approx (k_{\text{CI}})_{\text{H}}$ (Figure 2). Transfer of ^1H from TIM to solvent D_2O (k_{ex}) is therefore too slow relative to turnover to allow the H- and D-labeled enzymes to approach equilibrium with solvent.²³

(2) The direct transfer of tritium from TIM to solvent was preferred over the initial transfer of the tritium label to a pool of hydrons at the enzyme active site.²⁵ However, if the hydron were transferred directly to solvent, then exchange of hydron between enzyme and solvent should be accelerated by general bases such as imidazole,²⁶ as has been well documented for carbonic anhydrase.²⁷ The constant yield of hydrogen-labeled product DHAP from the reaction of GAP in D_2O observed as the concentration of the basic form of imidazole buffer is increased from 0.014 to 0.56 M shows that there is no detectable buffer catalysis of the hydron exchange reaction with solvent.²⁸ Irwin Rose has provided evidence that hydron exchange is initially between the labeled acid and a pool of solvent water molecules at the enzyme active site, and that the final exchange reaction with bulk solvent occurs after dissociation of product.²⁹

(3) The simplifying assumption that isomerization proceeds through a single reaction intermediate was made.³⁰ This requires either enzyme-catalyzed isomerization of GAP and DHAP through a common enediol phosphate or that proton transfer between O-1 and O-2 of isomeric enediolate phosphate oxyanions (Figure 2) is fast relative to turnover, so that these anions are effectively at chemical equilibrium. However, we observe different product distributions from the partitioning of the intermediates generated from the TIM-catalyzed reactions of GAP [red products (Figure 2)] and of DHAP in D_2O (blue products).^{23,24} This requires different relative steady-state concentrations for the isomeric enediolate phosphate intermediates (Figure 2) during turnover of DHAP and GAP, in which case they cannot be at chemical equilibrium.

The simplifying assumptions described above are consistent with a solvent-exposed enzyme active site. They could be partly justified by the seemingly logical, but misguided, notion that there was no clear imperative for sequestering polar substrates at TIM from the polar solvent water, because water already provides strong stabilization of the transition states for polar reactions. Later X-ray crystallographic analyses showed that TIM binds substrate and other ligands at a solvent-exposed cavity, and that binding is followed by closure of loop 6 [residues 166–176 (Scheme 2)] over the phosphodianion, which sequesters the carbon acid from solvent.^{31–33} It is now understood that enzymatic catalysis of proton transfer at carbon is favored at solvent-occluded active sites, because of the enhancement of electrostatic interactions between charged

Scheme 2



transition states and polar side chains that occurs as the local active site dielectric constant is decreased below that for water.^{34,35} This includes the strengthening of simple electrostatic interactions along with the tightening of hydrogen bonds, which may take on the structure of low-barrier hydrogen bonds.^{36,37}

Phosphodianion Binding Energy. Pompliano and Knowles reasoned that deletion of residues 170–173 (green in Scheme 2 and Figure 3A) of loop 6 and the introduction of a peptide bond between A169 and K174 should disrupt loop–dianion interactions without significantly affecting the protein fold (Figure 3B).³² The large 10^5 -fold decrease in k_{cat} and the much smaller 2.3-fold increase in K_{m} determined for isomerization of GAP catalyzed by the loop deletion mutant (LDM) of TIM from chicken muscle (ϵTIM) provide strong evidence that the benefits of loop 6 closure far exceed any energetic costs, as suggested by Wolfenden in 1974.³⁸

The low catalytic activity of the LDM showed that interactions between the substrate and phosphodianion gripper loop 6 activate TIM for catalysis. This raises the question of the total contribution of protein–phosphodianion interactions to the enzymatic rate acceleration. Truncation of the dianion results in a large decrease in activity from a $k_{\text{cat}}/K_{\text{m}}$ of $10^8 \text{ M}^{-1} \text{ s}^{-1}$ for TIM-catalyzed isomerization of GAP³⁹ to $k_{\text{cat}}/K_{\text{m}}$ values of 0.34^{40} and $0.1 \text{ M}^{-1} \text{ s}^{-1}$,⁴¹ respectively, for the TIM-catalyzed reactions of D-glyceraldehyde (DGA) and $[1\text{-}^{13}\text{C}]\text{-glycolaldehyde}$ ($[1\text{-}^{13}\text{C}]\text{GA}$) in D_2O . A 12 kcal/mol intrinsic phosphodianion binding energy was calculated from the decrease in $k_{\text{cat}}/K_{\text{m}}$ for the whole compared to truncated substrates.⁴⁰ TIM-catalyzed deprotonation of DGA is only marginally faster than deprotonation catalyzed by the small general base catalyst 3-quinuclidinone ($k_{\text{B}} = 6.5 \times 10^{-3} \text{ M}^{-1} \text{ s}^{-1}$),⁴⁰ so that $\sim 80\%$ of the transition-state stabilization of this near-perfect enzyme is eliminated by truncation of the remote substrate phosphodianion group.⁴⁰ This is a profoundly significant result, because it shows that the characterization of the enzyme–phosphodianion interactions is central to the development of an understanding of the enzymatic rate acceleration.

A critical question is whether the TIM–phosphodianion interactions simply anchor GAP and DHAP to the enzyme or if they also activate TIM for catalysis of proton transfer. Cutting the connection between the carbon acid and phosphodianion allows the effect of the dianion interaction to be determined absent this anchor. A very large increase in $(k_{\text{cat}}/K_{\text{m}})_{\text{obs}}$ for TIM-catalyzed deuterium exchange reactions of GA in D_2O was observed as the concentration of phosphite dianion was increased (Scheme 3).⁴² The yields of the three products of HPO_3^{2-} -activated TIM-catalyzed reactions of $[1\text{-}^{13}\text{C}]\text{GA}$ in D_2O (Scheme 4) are similar to the yields of the corresponding products of the reactions of the whole substrates (Figure 2).⁴¹ The principal difference between the catalyzed reactions of the whole substrate and its pieces^{41–43} is the ~ 6 kcal/mol entropic advantage provided by connecting the pieces.⁴⁴ This connection allows triosephosphates to bind and react with the loss

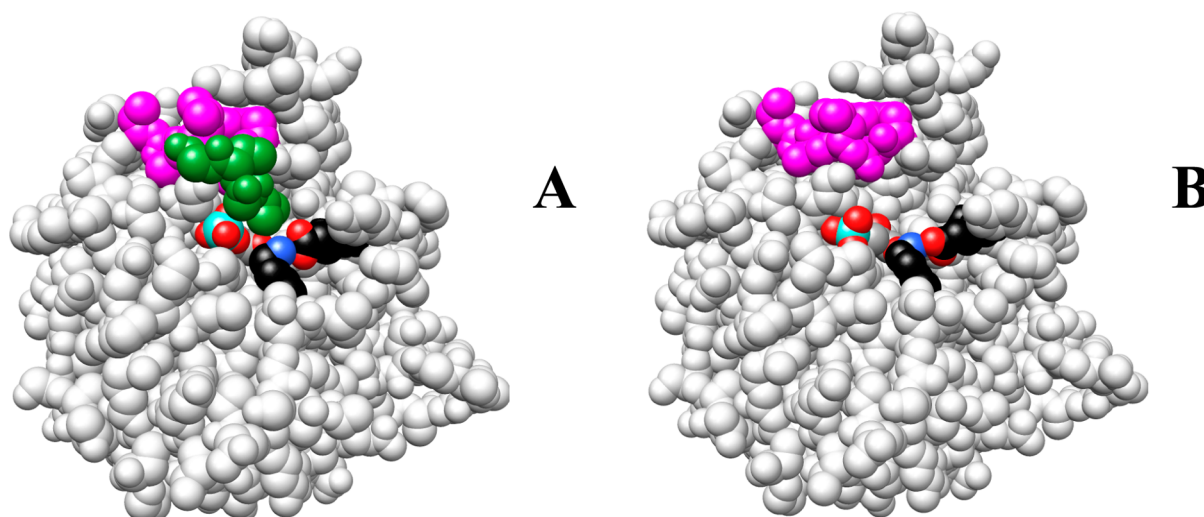
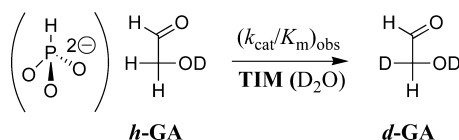
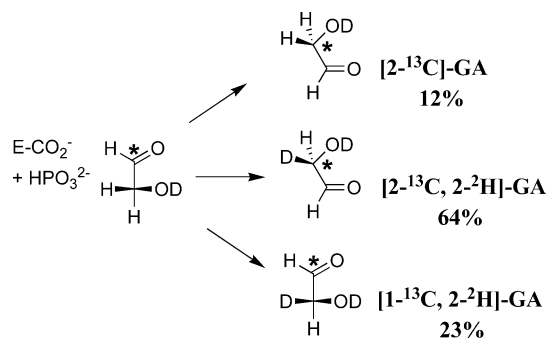


Figure 3. (A) Space filling model of the complex between TIM from yeast and PGA (PDB entry 2YPI).⁷³ The amino acid side chains of loop 6 that were kept for the LDM are colored magenta, and the deleted residues are colored green. The cationic side chain of K12 is shown on the left-hand side of the protein with the nitrogen (blue) in an ion pair to oxygen (red) of the anionic side chain of E97. (B) LDM of TIM generated from the structure for wild-type TIM (Figure 3A) by a procedure similar to that described for the K12G mutant of TIM from yeast.⁵³ The amino acid side chains of loop 6 that were preserved for the LDM are colored magenta.

Scheme 3



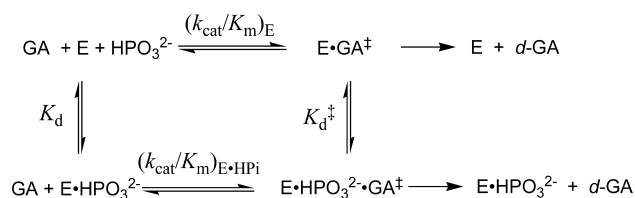
Scheme 4



of translational and rotational entropy of a single molecule, compared to the larger loss of entropy associated with the binding of the separate pieces, GA and HPO_3^{2-} .⁴⁵

An analysis of the dependence of $(k_{\text{cat}}/K_{\text{m}})_{\text{obs}}$ for rabbit muscle TIM-catalyzed reactions of GA in D_2O on HPO_3^{2-} concentration provided three kinetic parameters (Scheme 5): $(k_{\text{cat}}/K_{\text{m}})_{\text{E}} \approx 0.1 \text{ M}^{-1} \text{ s}^{-1}$ (this is smaller than an earlier published value of $0.26 \text{ M}^{-1} \text{ s}^{-1}$,⁴¹ which did not include the

Scheme 5



complete correction for a competing nonspecific deuterium exchange reaction that occurs outside the active site of TIM), $K_{\text{d}} = 38 \text{ mM}$ for binding of phosphite dianion, and $(k_{\text{cat}}/K_{\text{m}})_{\text{E} \cdot \text{Pi}} \approx 185 \text{ M}^{-1} \text{ s}^{-1}$.⁴² Similar kinetic parameters were determined for the reaction catalyzed by TIM from *Trypanosoma brucei* (*TbbTIM*).⁴³ The observed interaction between TIM and phosphite dianion is relatively weak [$\Delta G_{\text{obsd}} = RT \ln(0.038) = -1.9 \text{ kcal/mol}$]. The 1850-fold larger value of $k_{\text{cat}}/K_{\text{m}}$ for catalysis of deprotonation of GA by free enzyme E compared to $\text{E} \cdot \text{Pi}$ shows that these interactions strengthen to -6.4 kcal/mol [$K_{\text{d}}^\ddagger \approx 20 \text{ } \mu\text{M}$ (Scheme 5)] at the $\text{E} \cdot \text{GA}^\ddagger \cdot \text{Pi}$ transition-state complex.

An engineered monomeric variant of *TbbTIM* (mono-TIM)⁴⁶ catalyzes isomerization of GAP with a $k_{\text{cat}}/K_{\text{m}}$ of $1000 \text{ M}^{-1} \text{ s}^{-1}$,⁴³ which is similar to the $k_{\text{cat}}/K_{\text{m}}$ for isomerization of xylose catalyzed by xylose isomerase (XI)⁴⁷ but much smaller than the $k_{\text{cat}}/K_{\text{m}}$ of $10^7 \text{ M}^{-1} \text{ s}^{-1}$ for wild-type *TbbTIM*.⁴³ MonoTIM shows no detectable phosphite activation.⁴³ Apparently, respectable catalysis of isomerization of GAP is possible for the monomeric enzyme, but the functioning catalytic machinery that results in phosphite dianion activation is critical to achieving perfection in catalysis of the isomerization reaction.⁷

We have examined three enzymes that utilize a phosphodianion gripper loop: TIM, orotidine 5'-monophosphate decarboxylase,⁴⁸ and α -glycerol phosphate dehydrogenase.⁴⁹ In each case, (a) a total intrinsic phosphodianion binding energy of 12 kcal/mol was determined from the ratio of second-order rate constants ($k_{\text{cat}}/K_{\text{m}}$) for the enzyme-catalyzed reactions of whole and dianion-truncated substrates and (b) roughly half of this binding energy was observed in phosphite dianion activation of the enzyme-catalyzed reactions of the respective truncated substrates. The striking similarity of these results for enzymes that utilize phosphodianion gripper loops in catalysis of proton transfer, hydride transfer, and decarboxylation reactions of phosphorylated substrates is consistent with the notion that a common general mechanism has evolved for using dianion binding interactions to activate enzymes for catalysis.

Phosphodianion Binding Interactions. The X-ray crystal structure of the complex between TIM and the intermediate analogue PGH⁵⁰ shows that the 12 kcal/mol intrinsic phosphodianion binding energy is due partly or entirely to hydrogen bonding interactions of the phosphodianion with the backbone amides of Gly-171 (loop 6), Ser-211 (loop 7), and Gly-232 and -233 (loop 8) and to an ionic interaction with the cationic side chain of Lys-12. Loop 6 and the side chain K12 lie next to one another on the protein surface (Figure 3A). In addition to the isomerization reaction, the LDM⁵² and K12G mutant⁵¹ of TIM catalyze the elimination reaction of triosephosphates to form methylglyoxal and phosphate. Therefore, loop 6 and the cationic side chain of K12 operate in concert to slow the otherwise fast breakdown of the O-1 oxanyan enediolate phosphate intermediate.^{16,52}

It is difficult to account for the large 6×10^5 -fold effect of the K12G mutation on k_{cat}/K_m ⁵³ by the loss of ion pairing/hydrogen bonding interactions of the cationic side chain of K12, and even harder to account for the 10^5 -fold effect of the LDM (Figure 3B) on k_{cat} for isomerization of GAP³² by the loss of the single backbone hydrogen bond (Gly-171) between the phosphodianion and loop 6. We suggest that these catalytic elements act cooperatively to stabilize the transition state for substrate deprotonation, so that the elimination of a single element by the LDM or K12G mutation leads to a partial or full loss of the transition-state stabilization from the second element.

Figure 4A shows a view from the protein interior of the interaction between the side chain of K12 and the phosphodianion of DHAP.⁵⁴ The alkylammonium cation lies roughly equidistant from the phosphodianion and carbonyl groups of bound DHAP and interacts with both centers. With the movement from the Michaelis complex to the enediolate-like transition state for deprotonation of GAP, there is a change in the formal charge at the substrate carbonyl oxygen, from 0 to -1, and in the total charge at bound ligand, from -2 to -3. This increase in charge will result in an increase in the strength of the stabilizing electrostatic interactions between the alkylammonium side chain of Lys-12 and the transition state; it was proposed to account for the $\sim 10^4$ -fold effect of this mutation on k_{cat} for isomerization of GAP.⁵¹ An important effect of closure of loop 6 is the partial desolvation of the enzyme active site.³¹ This results in a reduction in the local dielectric constant of the active site that will lead to a strengthening of the stabilizing interactions between polar side chains and the transition state.⁵⁵ A tightening of polar interactions, including the ion pairing interaction to the side chain of K12, that is the result of loop closure will increase the driving force for closure. This global effect of loop closure on electrostatic and hydrogen bonding interactions may be the reason why the 7 kcal/mol effect of the LDM on the stability of the transition state for isomerization is so much greater than that any reasonable estimate of the strength of the single loop-dianion interaction eliminated by the LDM.³²

Chemical Reaction Mechanism. Questions continue to be raised about the elegant chemical mechanism for TIM (Figure 1) proposed by Knowles and co-workers.^{14,15} Balaram et al. have proposed that the side chain of K12 rather than H95 functions to protonate O-2 of DHAP by a mechanism that “eliminates the need to invoke the formation of the energetically unfavorable imidazolite anion at H95”.⁵⁶ We note the following observations that strongly support the mechanism of Knowles and co-workers (Figure 1), where the

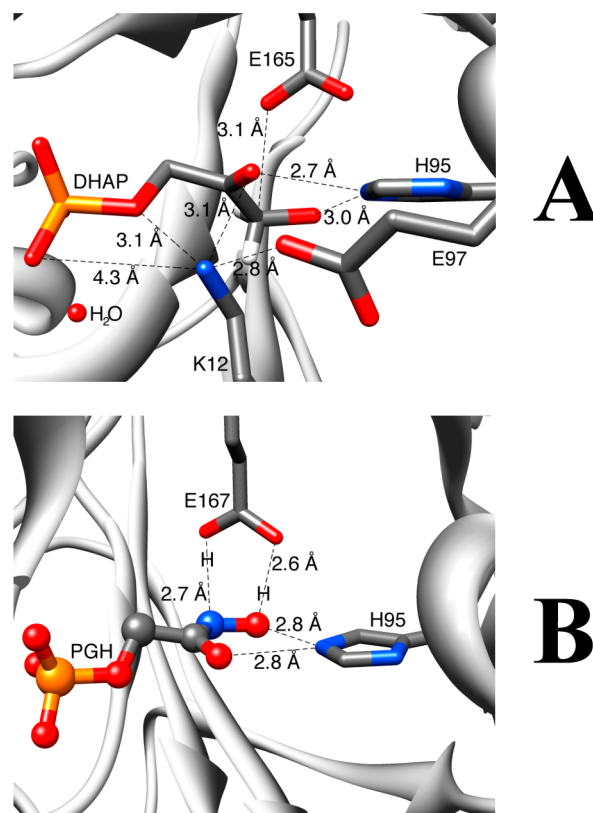


Figure 4. (A) Active site of TIM, taken from the X-ray crystal structure of McDermott and co-workers (PDB entry 1NEY),⁵⁴ showing the distances between the ammonium nitrogen of Lys-12 and the functional groups of bound substrate DHAP. (B) The 0.82 Å resolution structure of the complex between TIM (*L. mexicana*) and the enediolate intermediate analogue PGH (PDB entry 2VXN)⁶² showing the distances from the catalytic side chains to the ligand.

imidazole side chain of H95 functions as an electrophile in the stabilization of negative charge at isomeric enediolate phosphate intermediates.

(1) Formation of imidazolite anion at H95 is not strongly energetically unfavorable! The pK_a of ~ 14 ⁵⁷ for deprotonation of neutral imidazole in water is marginally higher than the pK_a of ~ 10 for a simple alkylammonium cation; however, the architecture of the active site of TIM favors a reversal in these relative pK_a values. The pK_a of ~ 14 for the neutral side chain of imidazole should be decreased at the protein because of an interaction with the positive end of a short α -helix that stabilizes the imidazole anion,^{15,58} and the pK_a of ~ 10 for the ammonium cation is increased because of stabilization of this cation by its ion pairing to the carboxylate side chain of Glu-97.

(2) Protonation of the carboxylate side chain of E97, a step in the mechanism proposed by Balaram and co-workers, should not be a part of the catalytic cycle for TIM. The X-ray crystal structure of E97Q mutant TIM shows dramatic movement of the K12 side chain away from substrate.⁵⁶ This is one consequence of the loss of the ion pair between K12 and E97 (Figure 4A) and contributes to the large 4000-fold decrease in k_{cat} for E97Q TIM-catalyzed isomerization of GAP.⁵⁶ The neutral E97 side chain of wild-type TIM, $-\text{CH}_2\text{CH}_2\text{C}(\text{O})\text{OH}$, resembles the neutral $-\text{CH}_2\text{CH}_2\text{C}(\text{O})\text{NH}_2$ side chain of the E97Q mutant. The conversion of the wild-type side chain anion to the neutral form should therefore cause a

conformational change and decrease in catalytic activity similar to that observed for E97Q mutant TIM.

(3) An atomic level X-ray crystal structure (0.82 Å resolution) of the enzyme-PGH complex for TIM from *Leishmania mexicana* shows that the hydroxamate oxygens form a bifurcated hydrogen bond to the NH group of H95 (Figure 4B). This structure of an enediolate analogue complex strongly implicates H95 in the stabilization of negative charge at both O-1 and O-2 of the isomeric enediolate phosphate oxyanion intermediates generated by deprotonation of GAP and DHAP, respectively (Figure 2), and in mediating the transfer of protons among these oxygen atoms.

X-ray crystal structures of TIM show an ion pair between the side chains of K12 and E97 (Figure 4A). One role for this ion pair is to immobilize the side chain of K12. This minimizes the decrease in entropy due to the loss of local translational and internal rotational motions that would occur if a flexible side chain were to form an ion pair to the transition state for the isomerization reaction.⁵¹ The formation of ion pairs between the anionic side chain of E97 and exogenous ammonium cations at K12G mutant yeast TIM is probably critical to the ability of these cations to rescue a substantial portion of the activity of the wild-type enzyme.⁵³

Phosphite Activation. If Eyring transition-state theory holds for the reactions of small molecules in water and at enzyme active sites, then the underlying cause of enzymatic catalysis is the stabilization of the transition state by strong “binding” interactions with the protein catalyst.⁵⁹ This total transition-state stabilization is often so large that it cannot be expressed entirely at the Michaelis complex, because this would result in effectively irreversible ligand binding and strongly rate-determining product release.⁶⁰ Enzymes therefore show specificity in binding their transition states with higher affinity than substrate. We consider now the molecular explanation for the specificity of TIM toward binding the isomerization transition state.

Between 4 and 5 of the total 12 kcal/mol intrinsic phosphodianion binding energy is expressed as phosphite dianion activation of TIM for catalysis of the reactions of $[1-^{13}\text{C}]\text{GA}$.^{42,43} This binding energy cannot be utilized to anchor the carbon acid substrate GA to TIM (K_m effect) and must therefore be specifically expressed at the transition state (k_{cat} effect) for the TIM-catalyzed reactions of GA and, by analogy, at the transition state for TIM-catalyzed reactions of the whole substrates GAP and DHAP.

The large difference between the K_d of 38 mM and the K_d^\ddagger of $\approx 20 \mu\text{M}$ (Scheme 5) for binding of HPO_3^{2-} to free TIM and $\text{E}\cdot\text{GA}^\ddagger$, respectively, might reflect a direct interaction between the pieces that stabilizes the ternary complex. However, the anionic enediolate-like transition state for TIM-catalyzed deprotonation of GA^\ddagger should show unfavorable electrostatic interactions with bound phosphite dianion. Scheme 6 presents a mechanism for the activation of TIM by HPO_3^{2-} .⁴¹ TIM is proposed to exist in two forms: a dominant inactive loop open

enzyme E_O with a low affinity for ligand binding and a rare active loop-closed enzyme $[\text{E}_\text{C}; K_\text{C} \ll 1 \text{ (Scheme 6)}]$ that shows specificity in binding to phosphite dianion and to the transition-state GA^\ddagger . The binding of HPO_3^{2-} is weak and the TIM-catalyzed reaction of GA slow because the concentration of the closed enzyme E_C is low, so that a substantial portion of the ligand binding energy is used to drive the unfavorable conformational change. For example, only 1.9 of the total 6.4 kcal/mol phosphite dianion binding energy is observed upon formation of the Michaelis complex (Figure 5A). Once the energetic price for loop closure is paid, the full intrinsic ligand binding energy is expressed on binding of the second ligand, either HPO_3^{2-} or GA^\ddagger , to form the ternary $\text{E}\cdot\text{GA}^\ddagger\cdot\text{HPO}_3^{2-}$ complex (Figure 5A).

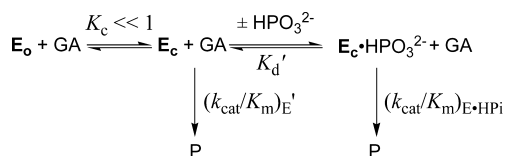
Scheme 6 assumes that there is a significant difference in the energy of E_O and E_C and in the reactivity of these different enzyme forms toward deprotonation of bound substrate. Six water molecules lie within 5 Å of the side chain of the catalytic base Glu-167 at unliganded *Tbb*TIM.⁶¹ The closure of loop 6 over bound ligands occludes bulk solvent and displaces several water molecules from the active site. Only two waters lie within 5 Å of the side chain of Glu-167 at the complex between TIM (*L. mexicana*) and PGH.⁶² The stripping of the polar solvent water from the active site (desolvation) should result in an increase in the energy of E_C compared to that of E_O .

X-ray crystal structures show that ligand-driven closure of loop 6 results in displacement of the carboxylate side chain of the active site base by several angstroms toward the ligand. The carboxylate oxygen of Glu-165 lies only 3.0 Å from the ketone and α -hydroxy carbons of DHAP in a high-resolution (1.2 Å) crystal structure of *c*TIM.⁵⁴ Preorganization of this basic side chain may facilitate transfer of a hydron from C-1 of DHAP to TIM. This proposal is supported by circumstantial evidence that small shifts in the position of the side chain in mutant forms of TIM are associated with substantial reductions in catalytic activity. For example, a comparison of X-ray crystal structures of *c*TIM-PGH complexes shows the carboxylate group of the catalytic base shifted by 0.7 Å (E165D⁶³) and 0.4 Å (S96P⁶⁴) from its position in wild-type *c*TIM. The E165D⁶⁵ and S96P⁶⁶ mutations cause 240- and 11-fold decreases, respectively, in k_{cat} for wild-type TIM and a <2-fold increase in K_m . It was also proposed that these mutations result in changes in the positioning of waters at the active site that affect catalytic activity.⁶⁴

Wierenga's lucid analysis of the changes in protein structure that occur during the ligand-gated loop closure⁸ brings to mind a precision mechanical device, such as a Swiss watch. Loop closure drives the hydrophobic side chain of Ile-172 of *Tbb*TIM toward the carboxylate side chain of Glu-167, and this “pushes” the side chain anion toward the second immobile hydrophobic side chain of Leu-232 (Figure 6).⁶⁷ This conformational change sandwiches the carboxylate side chain between two hydrophobic side chains and shields it from interactions with bulk solvent. “Hydrophobic clamping” should lead to an increase in the basicity of the carboxylate anion and, hence, in its reactivity toward deprotonation of carbon.

We have probed the role of I172 and L232 in activation of *Tbb*TIM for deprotonation of carbon. The I172A mutation results in a 200-fold decrease in k_{cat} for isomerization of the whole substrate GAP, but only a small <2-fold change in K_m .⁶⁸ The I172A mutant shows no detectable activity toward deprotonation of $[1-^{13}\text{C}]\text{GA}$: this corresponds to a >10-fold decrease in $(k_{\text{cat}}/K_m)_\text{E}$ (Scheme 5). The mutation results in a

Scheme 6



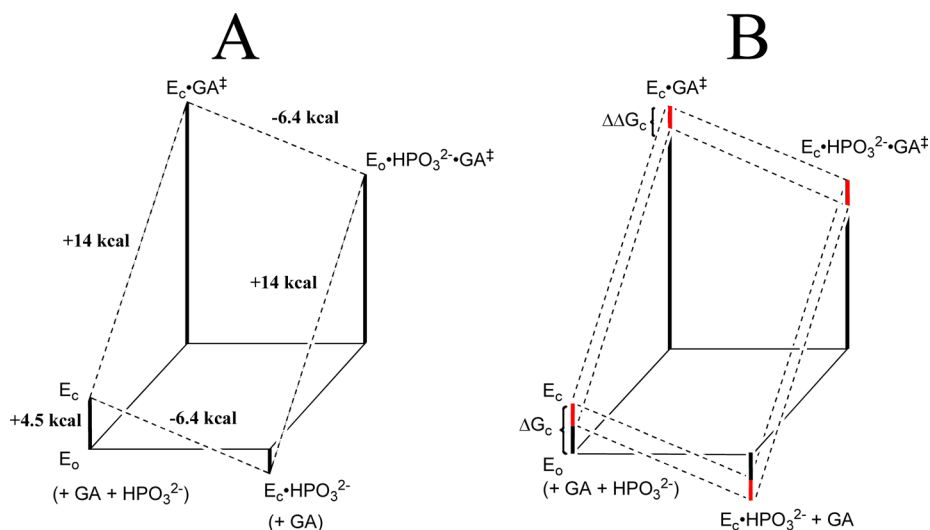


Figure 5. (A) Free energy profile for turnover of GA by free TIM (E_0) and by TIM that is saturated with phosphite dianion ($E_C \cdot \text{HPO}_3^{2-}$) that shows activation free energy changes calculated using the Eyring equation at 298 K. The difference between the total intrinsic phosphite binding energy of -6.4 kcal/mol and a ΔG° of -1.9 kcal/mol for binding of HPO_3^{2-} to the inactive open ground-state enzyme E_0 to give the active closed liganded enzyme $E_C \cdot \text{HPO}_3^{2-}$ is attributed to a ΔG_C of 4.5 kcal/mol for an unfavorable conformational change that converts E_0 to E_C . The observed value of ΔG^\ddagger (18.5 kcal/mol) for turnover of GA may be partitioned conceptually into a ΔG^\ddagger of 14 kcal/mol for proton transfer catalyzed by E_C and a ΔG_C of 4.5 kcal/mol for the obligate conformational change that converts E_0 to E_C . (B) Free energy profile that shows the effect of the L232A mutation on the kinetic parameters of wild-type *Tbb*TIM-catalyzed reactions of the substrate pieces. The red bars show the proposed effect of the L232A mutation on the barrier for the conformational change from E_0 to E_C ($\Delta\Delta G_C$). The effect of this change in ΔG_C on the turnover of the substrate pieces is shown by a comparison of the reaction profiles for wild-type TIM (top dashed lines) and L232A mutant TIM (bottom dashed lines).

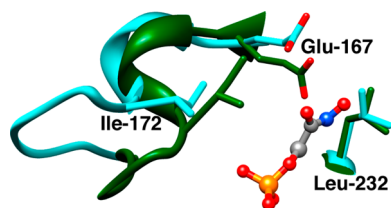


Figure 6. Superposition of models, from X-ray crystal structures, of the unliganded open (cyan, PDB entry 5TIM) and the PGH-liganded closed (green, PDB entry 1TRD) forms of *Tbb*TIM in the region of the enzyme active site. Closure of loop 6 (residues 168–178) over the ligand phosphodianion group shifts the hydrophobic side chain of Ile-172 toward the carboxylate side chain of the catalytic base Glu-167. This is accompanied by movement of Glu-167 toward the hydrophobic side chain of Leu-232, which maintains a nearly fixed position.

large 300-fold decrease in $(k_{\text{cat}}/K_m)_{E \cdot P_i}$, but there is little change in K_d for binding of phosphite dianion compared with wild-type *Tbb*TIM.⁶⁸ These results show that the hydrophobic side chain of I172A plays no role in the stabilization of the Michaelis complex to GAP or phosphite dianion, and a significant role in effecting the stabilization of the transition states for the wild-type TIM-catalyzed reactions of GAP and the substrate pieces. They provide support for the proposal that the hydrophobic clamping that accompanies loop closure⁶⁷ has the effect of enhancing the reactivity of the side chain of Glu-167 toward deprotonation of bound substrates (Figure 6).

The side chain of L232, which is contained in loop 8, remains nearly fixed during loop closure. The L232A mutation causes a small 6-fold decrease in k_{cat}/K_m for the *Tbb*TIM-catalyzed isomerization of GAP to give DHAP. We were surprised to observe that this mutation leads to an increase in the enzymatic activity toward catalysis of the reaction of the substrate pieces.⁶⁸ $(k_{\text{cat}}/K_m)_E$ for deprotonation of $[1\text{-}^{13}\text{C}]\text{GA}$ and dissociation

constant K_d for HPO_3^{2-} undergo a 17-fold increase and a 16-fold decrease compared to those of wild-type TIM, respectively (Scheme 5). On the other hand, similar values of $(k_{\text{cat}}/K_m)_{E \cdot P_i}$ are observed for the wild-type and L232A mutant enzymes.⁶⁹ The net effect of the L232A mutation is therefore to enhance the activity of the free enzyme, but not the activity of the $E \cdot P_i$ complex, toward deprotonation of $[1\text{-}^{13}\text{C}]\text{GA}$. The result is a stronger activation of the wild type than of the L232A mutant enzyme-catalyzed reactions by the binding of HPO_3^{2-} .

The critical observation of a 17-fold increase in $(k_{\text{cat}}/K_m)_E$ for the (supposedly crippled) L232A mutant enzyme-catalyzed reaction of $[1\text{-}^{13}\text{C}]\text{GA}$ is in keeping with our proposal that a portion of the ligand binding energy for wild-type TIM is used to drive an unfavorable conformational change. The higher activity for L232A mutant TIM can be rationalized by a decrease in the barrier to this conformational change [increase in K_C (Scheme 6)], in which case a larger fraction of the ligand binding energy will be observed as stabilization of the transition state for the L232A mutant TIM-catalyzed reaction of $[1\text{-}^{13}\text{C}]\text{GA}$. Specifically, the L232A mutation is proposed to cause an ~ 17 -fold increase in K_C for the thermodynamically unfavorable conversion of an inactive loop open form of TIM (E_0) to a higher-energy, but active, loop closed enzyme (E_C), which corresponds to a 1.7 kcal/mol change in ΔG_C .

Figure 5B illustrates the effect of a decrease in ΔG_C on the kinetic parameters for the TIM-catalyzed reactions of the substrate pieces. The proposed barrier to conversion of E_0 to E_C ($\Delta G_C = 4.5$ kcal/mol) for wild-type *Tbb*TIM is given by the sum of the red and black bars in the lower left-hand corner of Figure 5B. The red bars show the magnitude of the effect of the L232A mutation on this barrier ($\Delta\Delta G_C \approx 1.7$ kcal/mol). The barrier to ΔG_C is included in the barriers to formation of both the binary and ternary complexes (Figure 5B). Therefore, a decrease in ΔG_C would result in an increase in $(k_{\text{cat}}/K_m)_E$ (17-

fold), a decrease in K_d (16-fold), and an increase in $(k_{cat}/K_m)_E/K_d$ (25-fold). The magnitude of the activation of TIM for deprotonation of GA by the binding of phosphite dianion is determined by the magnitude of ΔG_c and will therefore decrease.

Panels A and B of Figure 5 provide a framework for interpreting the effect of the L232A mutation on the kinetic parameters for the TIM-catalyzed reactions of whole and truncated substrates. However, this model needs to be expanded and refined, and there is of course the need for additional experimental work.

(1) The model predicts that an increase in K_c results in an increase in the kinetic parameters for the substrate pieces that react specifically with the closed enzyme E_C . However, this change cannot cause an increase in k_{cat}/K_m for isomerization of the whole substrate GAP, because this reaction is already diffusion-limited.⁷⁰ The small 6-fold decrease in k_{cat}/K_m for isomerization of the whole substrate GAP by the L232A mutant cannot be rationalized by an increase in E_C concentration relative to E_O concentration. This effect might reflect small shifts in the position of the active site catalytic residues at the L232A mutant that lead to a decrease in the level of stabilization of the transition state for the reaction of the whole substrate GAP or DHAP, but not for the $GA + HPO_3^{2-}$ reaction, because cutting the covalent connection allows for independent movement of the pieces to their most reactive conformations at the active site.

(2) We envisioned similar functions for the hydrophobic side chains of I172 and L232 in desolvation of the basic side chain of E167, and in clamping this side chain next to the carbon acid substrate. However, mutations of I172 and L232 result in different changes in kinetic parameters. The I172A substitution causes a decrease in the reactivity of TIM for deprotonation of the whole substrate and the substrate pieces.⁶⁸ Apparently, the interactions between the mobile side chains of E167 and I172 function to activate TIM for deprotonation of the bound substrate. The L232A substitution causes a surprising increase in the kinetic parameter for catalysis of deprotonation of GA. Now, unfavorable interactions between E167 and the fixed side chain of L232 that develop upon loop closure are suggested to destabilize E_C , so that stabilization of E_C by interaction with phosphite dianion activates TIM for catalysis.

(3) It is important to consider the evolutionary force(s) that might select for a catalyst that exists predominately as a form that is inactive [E_O (Scheme 6)]. We suggest that this is partly or entirely due to the requirement that enzyme active sites be solvent-exposed to allow for substrate binding, and the catalytic advantages (see above) that arise from thermodynamically unfavorable active site desolvation during conversion of E_O to E_C . Note that the requirement for an unfavorable conformational change will not affect k_{cat}/K_m for turnover of GAP as long as the substrate reaction remains diffusion-limited. This is the case when the chemical steps are fast, and loop closure over GAP is thermodynamically favorable and faster than release of substrate to water. The phosphite dianion binding energy that is utilized to drive the conversion of E_O to E_C is not expressed at the Michaelis complex. This is required to avoid very tight ligand binding and strongly rate determining product release.⁶⁰

Concluding Remarks. The focus of classical kinetic studies of enzyme-catalyzed reactions is the determination of various kinetic parameters that define the relative stability of the free enzyme, Michaelis complexes, and the reaction transition state. These studies do not provide information about the changes in

protein structure that occur on proceeding first to the Michaelis complex and then to the transition state. These changes need to be considered when interpreting kinetic data, for example, the large conformational changes of TIM observed upon ligand binding.⁷¹ It is unclear whether the rate acceleration for TIM is enhanced by any requirement for the coupling of these protein motions to the chemical steps for the catalyzed reaction.⁷² However, at our modest empirical level, the rate acceleration of TIM-catalyzed isomerization can be accounted for by a consideration of the stabilizing interactions between the protein catalyst and transition state for deprotonation of α -carbonyl carbon.

AUTHOR INFORMATION

Corresponding Author

*Telephone: (716) 645-4232. Fax: (716) 645-6963. E-mail: jrichard@buffalo.edu.

Funding

This work was supported by Grant GM39754 from the National Institutes of Health.

Notes

The authors declare no competing financial interest.

ABBREVIATIONS

TIM, triosephosphate isomerase; *Tbb*TIM, TIM from *T. brucei*; *c*TIM, TIM from chicken muscle; monoTIM, engineered monomeric variant of *Tbb*TIM; LDM, loop deletion mutant of TIM; XI, xylose isomerase; DHAP, dihydroxyacetone phosphate; *d*-DHAP, [1(R)-²H]-dihydroxyacetone phosphate; GAP, (R)-glyceraldehyde 3-phosphate; *d*-GAP, [2(R)-²H]glyceraldehyde 3-phosphate; DGA, D-glyceraldehyde; GA, glycolaldehyde; NMR, nuclear magnetic resonance; NADH, nicotinamide adenine dinucleotide, reduced form; NAD, nicotinamide adenine dinucleotide, oxidized form; PDB, Protein Data Bank; PGH, 2-phosphoglycolohydroxamate; PGA, 2-phosphoglycolate.

REFERENCES

- (1) Hayden, E. C. (2008) Chemistry: Designer debacle. *Nature* 453, 275–278.
- (2) Rieder, S. V., and Rose, I. A. (1959) Mechanism of the triose phosphate isomerase reaction. *J. Biol. Chem.* 234, 1007–1010.
- (3) Shonk, C. E., and Boxer, G. E. (1964) Enzyme patterns in human tissues. I. Methods for the determination of glycolytic enzymes. *Cancer Res.* 24, 709–721.
- (4) Webster, K. A. (2003) Evolution of the coordinate regulation of glycolytic enzyme genes by hypoxia. *J. Exp. Biol.* 206, 2911–2922.
- (5) Richard, J. P., and Amyes, T. L. (2001) Proton transfer at carbon. *Curr. Opin. Chem. Biol.* 5, 626–633.
- (6) Gerlt, J. A., Kozarich, J. W., Kenyon, G. L., and Gassman, P. G. (1991) Electrophilic Catalysis Can Explain the Unexpected Acidity of Carbon Acids in Enzyme-Catalyzed Reactions. *J. Am. Chem. Soc.* 113, 9667–9669.
- (7) Knowles, J. R., and Albery, W. J. (1977) Perfection in enzyme catalysis: The energetics of triosephosphate isomerase. *Acc. Chem. Res.* 10, 105–111.
- (8) Wierenga, R. K. (2010) Triosephosphate isomerase: A highly evolved biocatalyst. *Cell. Mol. Life Sci.* 67, 3961–3982.
- (9) Miller, J. C., and Waley, S. G. (1971) Active center of rabbit muscle triose phosphate isomerase. Site that is labeled by glycidol phosphate. *Biochem. J.* 123, 163–170.
- (10) Waley, S. G., Miller, J. C., Rose, I. A., and O'Connell, E. L. (1970) Identification of site in triose phosphate isomerase labeled by glycidol phosphate. *Nature* 227, 181.

- (11) Nickbarg, E. B., Davenport, R. C., Petsko, G. A., and Knowles, J. R. (1988) Triosephosphate isomerase: Removal of a putatively electrophilic histidine residue results in a subtle change in catalytic mechanism. *Biochemistry* 27, 5948–5960.
- (12) Lodi, P. J., Chang, L. C., Knowles, J. R., and Komives, E. A. (1994) Triosephosphate isomerase requires a positively charged active site: The role of lysine-12. *Biochemistry* 33, 2809–2814.
- (13) Joseph-McCarthy, D., Lolis, E., Komives, E. A., and Petsko, G. A. (1994) Crystal structure of the K12M/G15A triosephosphate isomerase double mutant and electrostatic analysis of the active site. *Biochemistry* 33, 2815–2823.
- (14) Knowles, J. R. (1991) Enzyme catalysis: Not different, just better. *Nature* 350, 121–124.
- (15) Knowles, J. R. (1991) To build an enzyme. *Philos. Trans. R. Soc. London, Ser. B* 332, 115–121.
- (16) Richard, J. P. (1984) Acid-base catalysis of the elimination and isomerization reactions of triose phosphates. *J. Am. Chem. Soc.* 106, 4926–4936.
- (17) Amyes, T. L., and Richard, J. P. (1992) Generation and stability of a simple thiol ester enolate in aqueous solution. *J. Am. Chem. Soc.* 114, 10297–10302.
- (18) Amyes, T. L., and Richard, J. P. (1996) Determination of the pK_a of ethyl acetate: Brønsted correlation for deprotonation of a simple oxygen ester in aqueous solution. *J. Am. Chem. Soc.* 118, 3129–3141.
- (19) Richard, J. P., Williams, G., and Gao, J. L. (1999) Experimental and computational determination of the effect of the cyano group on carbon acidity in water. *J. Am. Chem. Soc.* 121, 715–726.
- (20) Rios, A., Amyes, T. L., and Richard, J. P. (2000) Formation and stability of organic zwitterions in aqueous solution: Enolates of the amino acid glycine and its derivatives. *J. Am. Chem. Soc.* 122, 9373–9385.
- (21) Chaing, Y., Guo, H.-X., Kresge, A. J., Richard, J. P., and Toth, K. (2003) The Mandelamide Keto-Enol System in Aqueous Solution. Generation of the Enol by Hydration of Phenylcarbamoylcarbene. *J. Am. Chem. Soc.* 125, 187–194.
- (22) Richard, J. P., Williams, G., O'Donoghue, A. C., and Amyes, T. L. (2002) Formation and stability of enolates of acetamide and acetate anion: An Eigen plot for proton transfer at α -carbonyl carbon. *J. Am. Chem. Soc.* 124, 2957–2968.
- (23) O'Donoghue, A. C., Amyes, T. L., and Richard, J. P. (2005) Hydron Transfer Catalyzed by Triosephosphate Isomerase. Products of Isomerization of (R)-Glyceraldehyde 3-Phosphate in D_2O . *Biochemistry* 44, 2610–2621.
- (24) O'Donoghue, A. C., Amyes, T. L., and Richard, J. P. (2005) Hydron Transfer Catalyzed by Triosephosphate Isomerase. Products of Isomerization of Dihydroxyacetone Phosphate in D_2O . *Biochemistry* 44, 2622–2631.
- (25) Fisher, L. M., Albery, W. J., and Knowles, J. R. (1976) Energetics of triosephosphate isomerase: The nature of the proton transfer between the catalytic base and solvent water. *Biochemistry* 15, 5621–5626.
- (26) Eigen, M. (1964) Proton Transfer, Acid-Base Catalysis, and Enzymatic Hydrolysis. *Angew. Chem., Int. Ed.* 3, 1–72.
- (27) Tu, C., Paranawithana, S. R., Jewell, D. A., Tanhauser, S. M., LoGrasso, P. V., Wynns, G. C., Laipis, P. J., and Silverman, D. N. (1990) Buffer Enhancement of Proton Transfer in Catalysis by Human Carbonic Anhydrase III. *Biochemistry* 29, 6400–6405.
- (28) O'Donoghue, A. C., Amyes, T. L., and Richard, J. P. (2008) Slow proton transfer from the hydrogen-labelled carboxylic acid side chain (Glu-165) of triosephosphate isomerase to imidazole buffer in D_2O . *Org. Biomol. Chem.* 6, 391–396.
- (29) Rose, I. A., Fung, W. J., and Warms, J. V. B. (1990) Proton diffusion in the active site of triosephosphate isomerase. *Biochemistry* 29, 4312–4317.
- (30) Albery, W. J., and Knowles, J. R. (1976) Free-energy profile for the reaction catalyzed by triosephosphate isomerase. *Biochemistry* 15, 5627–5631.
- (31) Malabanan, M. M., Amyes, T. L., and Richard, J. P. (2010) A role for flexible loops in enzyme catalysis. *Curr. Opin. Struct. Biol.* 20, 702–710.
- (32) Pompliano, D. L., Peyman, A., and Knowles, J. R. (1990) Stabilization of a reaction intermediate as a catalytic device: Definition of the functional role of the flexible loop in triosephosphate isomerase. *Biochemistry* 29, 3186–3194.
- (33) Berlow, R. B., Igumenova, T. I., and Loria, J. P. (2007) Value of a Hydrogen Bond in Triosephosphate Isomerase Loop Motion. *Biochemistry* 46, 6001–6010.
- (34) Guthrie, J. P., and Kluger, R. (1993) Electrostatic Stabilization Can Explain the Unexpected Acidity of Carbon Acids in Enzyme-Catalyzed Reactions. *J. Am. Chem. Soc.* 115, 11569–11572.
- (35) Richard, J. P., and Amyes, T. L. (2004) On the importance of being zwitterionic: Enzymic catalysis of decarboxylation and deprotonation of cationic carbon. *Bioorg. Chem.* 32, 354–366.
- (36) Harris, T. K., Abeygunawardana, C., and Mildvan, A. S. (1997) NMR studies of the role of hydrogen bonding in the mechanism of triosephosphate isomerase. *Biochemistry* 36, 14661–14675.
- (37) Cleland, W. W., Frey, P. A., and Gerlt, J. A. (1998) The Low Barrier Hydrogen Bond in Enzymatic Catalysis. *J. Biol. Chem.* 273, 25529–25532.
- (38) Wolfenden, R. (1974) Enzyme catalysis. Conflicting requirements of substrate access and transition state affinity. *Mol. Cell. Biochem.* 3, 207–211.
- (39) Putman, S. J., Coulson, A. F. W., Farley, I. R. T., Riddleston, B., and Knowles, J. R. (1972) Specificity and kinetics of triose phosphate isomerase from chicken muscle. *Biochem. J.* 129, 301–310.
- (40) Amyes, T. L., O'Donoghue, A. C., and Richard, J. P. (2001) Contribution of phosphate intrinsic binding energy to the enzymatic rate acceleration for triosephosphate isomerase. *J. Am. Chem. Soc.* 123, 11325–11326.
- (41) Go, M. K., Amyes, T. L., and Richard, J. P. (2009) Hydron Transfer Catalyzed by Triosephosphate Isomerase. Products of the Direct and Phosphite-Activated Isomerization of [$1-^{13}C$]-Glycolaldehyde in D_2O . *Biochemistry* 48, 5769–5778.
- (42) Amyes, T. L., and Richard, J. P. (2007) Enzymatic catalysis of proton transfer at carbon: Activation of triosephosphate isomerase by phosphite dianion. *Biochemistry* 46, 5841–5854.
- (43) Malabanan, M. M., Go, M., Amyes, T. L., and Richard, J. P. (2011) Wildtype and Engineered Monomeric Triosephosphate Isomerase from *Trypanosoma brucei*: Partitioning of Reaction Intermediates in D_2O and Activation by Phosphite Dianion. *Biochemistry* 50, 5767–5769.
- (44) Jencks, W. P. (1981) On the attribution and additivity of binding energies. *Proc. Natl. Acad. Sci. U.S.A.* 78, 4046–4050.
- (45) Page, M. I., and Jencks, W. P. (1971) Entropic contributions to rate accelerations in enzymic and intramolecular reactions and the chelate effect. *Proc. Natl. Acad. Sci. U.S.A.* 68, 1678–1683.
- (46) Borchert, T. V., Abagyan, R., Jaenicke, R., and Wierenga, R. K. (1994) Design, creation, and characterization of a stable, monomeric triosephosphate isomerase. *Proc. Natl. Acad. Sci. U.S.A.* 91, 1515–1518.
- (47) Toteva, M. M., Silvaggi, N. R., Allen, K. N., and Richard, J. P. (2011) Binding Energy and Catalysis by D-Xylose Isomerase: Kinetic, Product, and X-ray Crystallographic Analysis of Enzyme-Catalyzed Isomerization of (R)-Glyceraldehyde. *Biochemistry* 50, 10170–10181.
- (48) Amyes, T. L., Richard, J. P., and Tait, J. J. (2005) Activation of orotidine 5'-monophosphate decarboxylase by phosphite dianion: The whole substrate is the sum of two parts. *J. Am. Chem. Soc.* 127, 15708–15709.
- (49) Tsang, W.-Y., Amyes, T. L., and Richard, J. P. (2008) A substrate in pieces: Allosteric activation of glycerol 3-phosphate dehydrogenase (NAD⁺) by phosphite dianion. *Biochemistry* 47, 4575–4582.
- (50) Zhang, Z., Sugio, S., Komives, E. A., Liu, K. D., Knowles, J. R., Petsko, G. A., and Ringe, D. (1994) Crystal Structure of Recombinant Chicken Triosephosphate Isomerase-Phosphoglycolohydroxamate Complex at 1.8-Å Resolution. *Biochemistry* 33, 2830–2837.

- (51) Go, M. K., Koudelka, A., Amyes, T. L., and Richard, J. P. (2010) Role of Lys-12 in Catalysis by Triosephosphate Isomerase: A Two-Part Substrate Approach. *Biochemistry* 49, 5377–5389.
- (52) Richard, J. P. (1991) Kinetic-parameters for the elimination reaction catalyzed by triosephosphate isomerase and an estimation of the reactions physiological significance. *Biochemistry* 30, 4581–4585.
- (53) Go, M. K., Amyes, T. L., and Richard, J. P. (2010) Rescue of K12G mutant TIM by NH_4^+ and alkylammonium cations: The reaction of an enzyme in pieces. *J. Am. Chem. Soc.* 132, 13525–13532.
- (54) Jogl, G., Rozovsky, S., McDermott, A. E., and Tong, L. (2003) Optimal alignment for enzymatic proton transfer: Structure of the Michaelis complex of triosephosphate isomerase at 1.2-Å resolution. *Proc. Natl. Acad. Sci. U.S.A.* 100, 50–55.
- (55) Hine, J. (1975) *Structural Effects on Equilibria in Organic Chemistry*, Wiley-Interscience, New York.
- (56) Samanta, M., Murthy, M. R. N., Balaram, H., and Balaram, P. (2011) Revisiting the Mechanism of the Triosephosphate Isomerase Reaction: The Role of the Fully Conserved Glutamic Acid 97 Residue. *ChemBioChem* 12, 1886–1895.
- (57) Yagil, G. (1967) Proton Dissociation Constant of Pyrrole Indole and Related Compounds. *Tetrahedron* 23, 2855.
- (58) Komives, E. A., Chang, L. C., Lolis, E., Tilton, R. F., Petsko, G. A., and Knowles, J. R. (1991) Electrophilic catalysis in triosephosphate isomerase: The role of histidine-95. *Biochemistry* 30, 3011–3019.
- (59) Pauling, L. (1948) Nature of forces between large molecules of biological interest. *Nature* 161, 707–709.
- (60) Jencks, W. P. (1975) Binding energy, specificity and enzymic catalysis: The Circe effect. *Adv. Enzymol. Relat. Areas Mol. Biol.* 43, 219–410.
- (61) Wierenga, R. K., Noble, M. E. M., Vriend, G., Nauche, S., and Hol, W. G. J. (1991) Refined 1.83 Å structure of trypanosomal triosephosphate isomerase crystallized in the presence of 2.4 M-ammonium sulfate. A comparison with the structure of the trypanosomal triosephosphate isomerase-glycerol-3-phosphate complex. *J. Mol. Biol.* 220, 995–1015.
- (62) Alahuhta, M., and Wierenga, R. K. (2010) Atomic resolution crystallography of a complex of triosephosphate isomerase with a reaction intermediate analog: New insight in the proton transfer reaction mechanism. *Proteins: Struct., Funct., Bioinf.* 78, 1878–1888.
- (63) Joseph-McCarthy, D., Rost, L. E., Komives, E. A., and Petsko, G. A. (1994) Crystal Structure of the Mutant Yeast Triosephosphate Isomerase in Which the Catalytic Base Glutamic Acid 165 Is Changed to Aspartic Acid. *Biochemistry* 33, 2824–2829.
- (64) Zhang, Z., Komives, E. A., Sugio, S., Blacklow, S. C., Narayana, N., Xuong, N. H., Stock, A. M., Petsko, G. A., and Ringe, D. (1999) The Role of Water in the Catalytic Efficiency of Triosephosphate Isomerase. *Biochemistry* 38, 4389–4397.
- (65) Straus, D., Raines, R., Kawashima, E., Knowles, J. R., and Gilbert, W. (1985) Active site of triosephosphate isomerase: In vitro mutagenesis and characterization of an altered enzyme. *Proc. Natl. Acad. Sci. U.S.A.* 82, 2272–2276.
- (66) Blacklow, S. C., and Knowles, J. R. (1990) How can a catalytic lesion be offset? The energetics of two pseudorevertant triosephosphate isomerases. *Biochemistry* 29, 4099–4108.
- (67) Kursula, I., and Wierenga, R. K. (2003) Crystal structure of triosephosphate isomerase complexed with 2-phosphoglycolate at 0.83-Å resolution. *J. Biol. Chem.* 278, 9544–9551.
- (68) Malabanan, M. M. Unpublished results.
- (69) Malabanan, M. M., Amyes, T. L., and Richard, J. P. (2011) Mechanism for Activation of Triosephosphate Isomerase by Phosphate Dianion: The Role of a Ligand-Driven Conformational Change. *J. Am. Chem. Soc.* 133, 16428–16431.
- (70) Blacklow, S. C., Raines, R. T., Lim, W. A., Zamore, P. D., and Knowles, J. R. (1988) Triosephosphate isomerase catalysis is diffusion controlled. *Biochemistry* 27, 1158–1165.
- (71) Rozovsky, S., Jogl, G., Tong, L., and McDermott, A. E. (2001) Solution-state NMR investigations of triosephosphate isomerase active site loop motion: Ligand release in relation to active site loop dynamics. *J. Mol. Biol.* 310, 271–280.
- (72) Desamero, R., Rozovsky, S., Zhadin, N., McDermott, A., and Callender, R. (2003) Active site loop motion in triosephosphate isomerase: T-Jump relaxation spectroscopy of thermal activation. *Biochemistry* 42, 2941–2951.
- (73) Olsson, M. H. M., Parson, W. W., and Warshel, A. (2006) Dynamical contributions to enzyme catalysis: Critical tests of a popular hypothesis. *Chem. Rev.* 106, 1737–1756.
- (74) Nagel, Z. D., and Klinman, J. P. (2009) A 21st century revisionists' view at a turning point in enzymology. *Nat. Chem. Biol.* 8, 543–550.
- (75) Lolis, E., and Petsko, G. A. (1990) Crystallographic analysis of the complex between triosephosphate isomerase and 2-phosphoglycolate at 2.5-Å resolution: Implications for catalysis. *Biochemistry* 29, 6619–6625.